A 2.5-to-4.5-GHz Switched-LC-Mixer-First Acoustic-Filtering RF Front-End Achieving <6dB NF, +30dBm IIP3 at 1×Bandwidth Offset

Hyungjoo Seo and Jin Zhou University of Illinois at Urbana-Champaign, Urbana, IL, 61801, USA

Abstract - This paper describes an agile RF front-end that consists of an N-path switched-LC mixer in silicon followed by an acoustic filter - essentially a mixer-first acoustic-filtering RF front-end. The mixer frequency-translates a sharp but fixed acoustic filtering profile to a much higher and LO-defined tunable frequency while preserves input matching, high-linearity, and introduces minimal loss. In contrast to the existing N-path passive-mixer-first receivers which use active baseband filters after N-path switches, using a single acoustic filter as the N-path load is fraught with fundamental challenges. We introduce on-chip LC-tanks to suppress the acoustic filter out-of-band impedance and an all-passive recombination network to share one acoustic filtering among N paths. A front-end prototype using a CMOS switched-LC passive mixer followed by an off-the-shelf 1.6-GHz surface-acoustic-wave (SAW) filter is designed and optimized. In measurement, the RF front-end operates across 2.5-to-4.5 GHz achieving 5.5-dB NF and +29.4-dBm IIP3 at 1×bandwidth offset.

I. INTRODUCTION

Tunable low-loss and high-linearity RF filters are essential for future software-defined and cognitive wireless networks that feature high spectral efficiency. In addition, as the number of cellular frequency bands keeps soaring, especially with the advent of sub-6-GHz 5G, a tunable RF filter can be employed to replace numerous fixed-frequency acoustic filters in a wireless transceiver.

Monolithic reconfigurable high-order band-pass filters using N-path switched-capacitor resonators have been reported recently [1], [2]. However, due to parasitic effects and the need of multi-phase square-wave RF clocks, these filters generally have limited out-of-band (OOB) rejection and do not perform well when operate beyond 3 GHz. Moreover, it should be noted that scaling acoustic filters or their filtering responses towards high frequencies is critical but fraught with challenges [3]. Mixer-first band-pass receivers that operate beyond 3 GHz have been reported (e.g. [4], [5]) but are power hungry when operated above 3 GHz and have limited suppression at close-in offset frequencies due to low-order filtering.

To enable frequency-tunable high-order filtering beyond 3 GHz, this paper describes a hybrid CMOS-acoustic filtering front-end solution (Fig. 1). It utilizes a single fixed-frequency high-order acoustic filter after an N-path switched-LC mixer. This way, interference at close-in offset frequencies is suppressed by the high-order acoustic filter while the front-end operation frequency is defined jointly by the mixer LO and the acoustic filter – essentially a mixer-first acoustic-filtering RF front-end. The linearity and power-handling of the proposed front-end is limited by the mixer. Therefore, a switched-LC

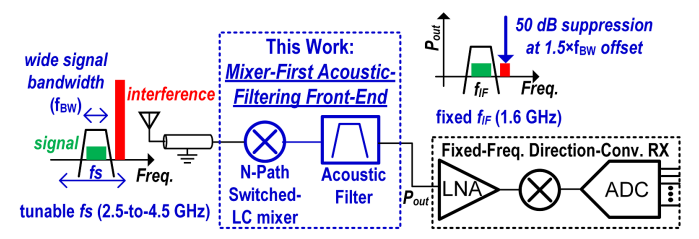


Fig. 1. Mixer-first acoustic-filtering agile front-end: conceptual diagram.

implementation without any active transistors is adopted in the signal path for high linearity.

When combined with a fixed-frequency direct-conversion receiver (Fig. 1), the proposed solution could cover multiple frequency bands, enabling software-defined and cognitive radios with superior interference tolerance in an increasingly congested and contested electromagnetic environment. When compared to the existing multi-band cellular front-end solutions, the proposed front-end design could significantly reduce the number of acoustic filters and on-chip receiver paths; it also could eliminate the need of a complex and lossy filter-bank switch at the antenna interface. A prototype using a CMOS switched-LC passive mixer followed by an off-the-shelf 1.6-GHz surface-acoustic-wave (SAW) filter is designed. In measurement, the RF front-end is continuously tunable across 2.5-to-4.5 GHz achieving 5.5-dB SSB NF and +29.4-dBm IIP3 at 1×bandwidth frequency offset. Thanks to a high intermediate frequency (IF) at 1.6 GHz, image signals are all below 1 GHz with 2.5-to-4.2-GHz RF. The mixer has >50 dB image rejection; even higher rejection can be obtained by an additional high-pass filter if needed.

II. DESIGN EVOLUTION AND CONSIDERATIONS

This section describes the design evolution leading to the switched-LC-mixer-first acoustic-filtering RF front-end as well as low-loss design considerations.

A. Switched-Band-Pass-Filter Mixer-First Frond-End

It is known that an N-path passive-mixer-first receiver has interesting properties of frequency-translational filtering and impedance translation [6], [7]. Figure 2(a) depicts an N-path switched-band-pass-filter mixer-first receiver where the switches (with switch resistance R_{SW}) act as a mixer that frequency-translates the desired signal to filter pass band and shifts the interference to stop band. A recombination network in the analog baseband (BB) sums the outputs from all paths for image and harmonic rejection [6], [7].

Similar to a switched-low-pass-filter mixer-first receiver (e.g. [6], [4], [5]), the receiver has a linear-time-invariant (LTI) equivalent model at the input frequency f_S . In this LTI model shown in Fig. 2(b), the load impedance at IF $Z_L(f_S-f_{LO})=Z_L(f_{IF})$ is translated to RF, where we've assumed that $2f_S$ and f_{LO} are incommensurable and $|Z_L(f)|$ has only a single peak, i.e. $|Z_L(f)|$ is negligible at harmonic frequencies f_S+pf_{LO} (p is an integer) except for p=-1. In Fig. 2(b), R_{sh} represents the losses from R_S and R_{SW} at harmonic frequencies [6]. With a large number of paths, it has been shown that input matching, negligible conversion loss/NF, and frequency-translational filtering can be achieved simultaneously; moreover, image/harmonic rejection can be obtained upon BB recombination [6], [7].

B. Suppressing Acoustic Filter OOB Impedance Peaks

One key challenge for using acoustic filters in an N-path receiver shown in Fig. 2(a) is the complexity of acoustic filter input impedance and the uncertainty associated with their interconnects to the silicon dies. A high-order acoustic band-pass filter with a sharp filtering profile usually consists of 5-20 resonators in SAW or bulk-acoustic-wave (BAW) technology, and hence its input impedance can have multiple peaks [8]. Simulated input impedance $|Z_L(f)|$ looking into a SAW filter using its measured S-parameters [9] and interconnects (consist of mixer chip parastic, 1-mm mixer chip bond wire, 2-mm on-board 50- Ω trace, and component pad) is depicted in Fig. 2(c). It shows non-negligible impedance at harmonic frequencies $f_S + p f_{LO}$ (except for p=-1), where $f_S - f_{LO} = f_{IF}$ =1.6 GHz and f_S =3.5 GHz.

Assuming a generic multi-peak IF load impedance $|Z_L(f)|$, the LTI input impedance model is modified and illustrated in Fig. 2(c). Simulation of input impedance Z_{in} versus f_S with a fixed 1.6-GHz $f_{IF} = f_S - f_{LO}$ validates the proposed generic LTI model. It can be seen that the non-negligible impedance at harmonic frequencies can hinder input matching and result in excessive losses dissipated in $Z_L(f+pf_{LO})$ (except for p=-1) and $R_{sh,p}$.

To lower Z_L at harmonic frequencies, we introduce on-chip LC tanks tuned at the desired IF right after the N-path switches (Fig. 3). Unlike the acoustic filter that suppresses close-in interference, the LC tanks provide low impedance at harmonic frequencies that are gigahertz away and hence can be realized with low-order on-chip implementations.

C. Single-Acoustic-Filter N-Path Filtering

Having on-chip LC-tanks right after the N-path switches allows us to have an all-passive recombination network early in the receiver chain at IF. This is because that the impedance at *harmonic frequencies* is dominated by the LC-tanks [Fig. 3(b)] and hence is immune to the impedance transformation associated with an all-passive recombination network which includes phase shifters and power combinators. This way, a single acoustic filter can be shared among N paths as illustrated in Fig. 4.

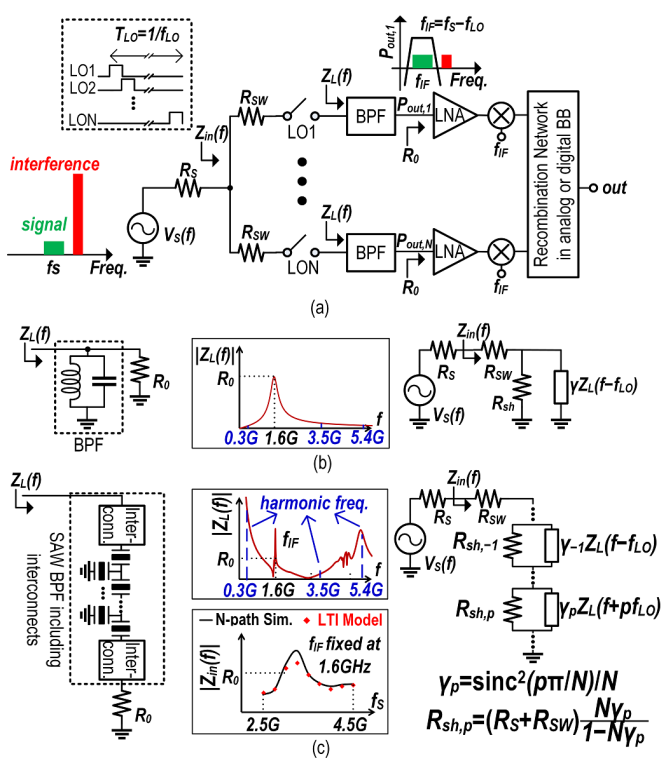


Fig. 2. Switched-band-pass-filter mixer-first frond-end: (a) receiver diagram; (b) with single-peak LC-BPF loads; and (c) with multi-peak acoustic-BPF and the interconnects between the acoustic and silicon dies.

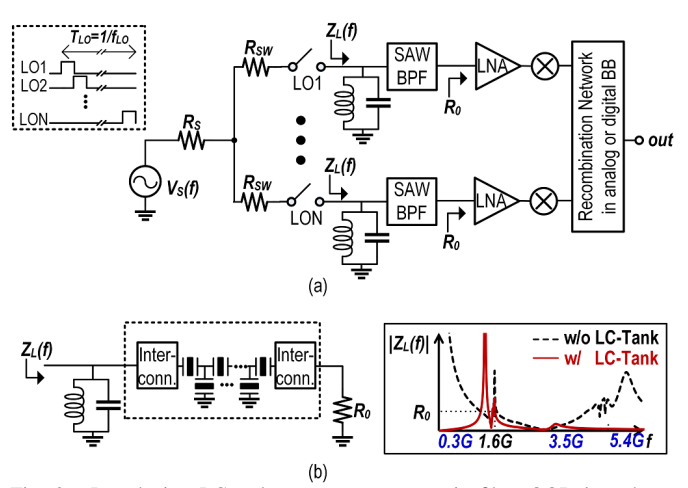


Fig. 3. Introducing LC-tanks to suppress acoustic filter OOB impedance: (a)receiver diagram; and (b) simulated impedance before and after suppression.

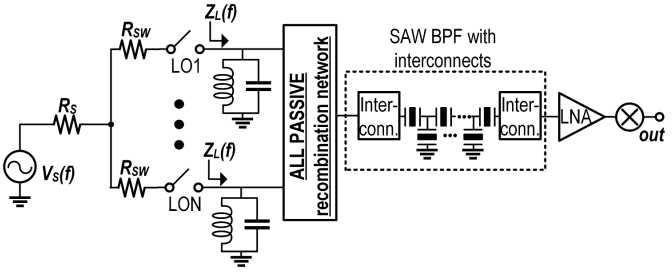


Fig. 4. Single-acoustic-filter N-path filtering using all-passive recombination network at IF.

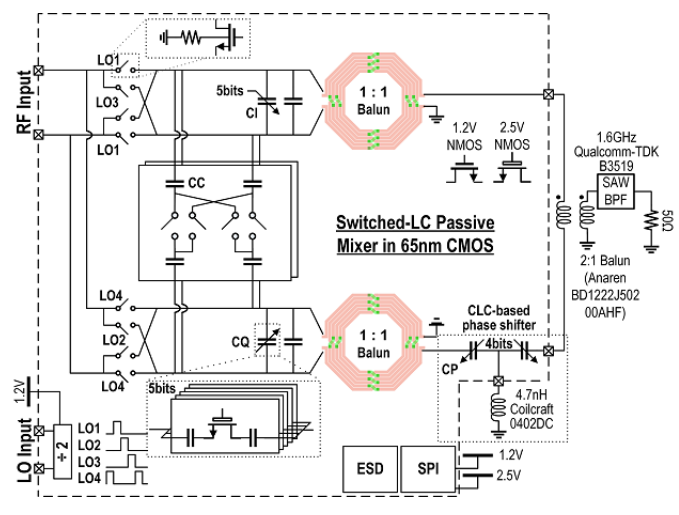


Fig. 5. Schematic of switched-LC mixer followed by a SAW filter.

Existing off-the-shelf acoustic filters are often designed to have $50-\Omega$ in-band (IB) resistance. However, when used in the proposed N-path front-end, the $50-\Omega$ resistance gets reduced significantly when it is translated from IF to RF. This necessitates some step-up impedance transformation. In our prototype implementation (see Fig. 5), a differential architecture helps us reduce the impedance transformation ratio from passive components approximately by $2\times$ thanks to its higher input resistance compared to a single-ended design.

D. Optimizing LC-Tank Q-Factor for Low Loss

There exists a design trade-off associated with the LC-tank Q-factor that affects the achievable loss in a practical design. The on-chip LC tanks (implemented as transformer baluns with digitally-controlled capacitor banks shown in Fig. 5) suppress the acoustic filter OOB impedance at harmonic frequencies. From this perspective, a higher tank Q-factor Q_T is preferable as it allows more suppression and hence lower mixing loss. However, a large Q_T leads to a small inductance L which results in a small unloaded LC-tank equivalent parallel resistance $R_P \approx \omega Q_S L$, where we've ignored the capacitor loss and Q_S is the inductor quality factor. For a low loss design, R_P needs to be much larger than the resistance (about 100 Ω) looking into the recombination network, resulting in a design requirement of small tank Q-factor $Q_T \ll Q_S$. In our design, a loaded LC-tank Q of 2-to-3 is chosen at 1.6 GHz, given Q_S of 13, to balance the mixing loss and the loss in the passive components. Lower loss can be achieved using a technology with better passives.

III. IMPLEMENTATION AND EXPERIMENTAL RESULTS

The proposed switched-LC mixer has been fabricated in a 65nm CMOS process. This chip is packaged and mounted on an FR4 PCB followed by a balun and a 1.6-GHz SAW filter [9] (Fig. 6). Similar to [1], [5], an off-chip balun (1:1) is used to facilitate single-ended measurements at input and its loss is de-embedded. N-path switches are designed to have an on-resistance of 5 Ω for low loss and their drain and source nodes are biased at 0.25 V while bulk nodes are tied to ground

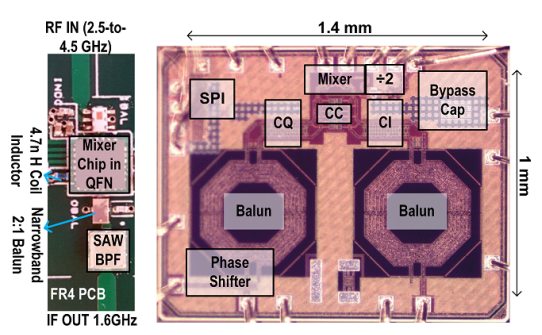


Fig. 6. Photographs of the RF front-end and the switched-LC mixer chip.

to tolerate large signals (Fig. 5). An on-chip divide-by-2 circuitry is used to generate the clocks driving the N-path switches. On-chip baluns provide inductive loads (about 5 nH) and act as parts of the all-passive recombination network. A CLC circuitry is employed in the recombination network to provide a 90° phase shift. All capacitors are realized as digitally-controlled capacitor banks using thick-oxide switches to compensate chip-and-board-level variations. Finally, direct and cross-coupled capacitor banks (C_C) are inserted between I/Q branches to compensate input impedance variation caused by parasitics or non-50-ohm antenna impedance.

The measured power-conversion gain and S11 of the mixer-first acoustic-filtering front-end is shown in Fig. 7 when the input is at 3.5 GHz (f_{LO} =1.9 GHz). The overall front-end loss is 5.6 dB including the loss of the mixer, output balun, and SAW filter as well as the package and PCB interconnect losses from the mixer input to the SAW filter output. A simulated loss distribution is also provided in Fig. 7. A stand-alone mixer from a separate testing PCB is also measured showing a loss of 4.3 dB. This deviates from our expected theoretical minimal loss of 1.1 dB for a 4-path mixer due to additional losses from switch parastics and on-chip baluns. Lower loss can be achieved using a technology with better switches and passives.

Across 2.5-to-4.5-GHz RF, power-conversion loss of 5.4-6.4 dB, SSB NF of 5.5-7.1 dB, and >50-dB image rejection are achieved in measurement (Fig. 8) with 12-26 mW power consumption from a 1.2 V supply. Thanks to the high IF at 1.6 GHz, image signals are all below 1 GHz with 2.5-to-4.2-GHz RF. Across the entire RF range, 40-to-50 dB stop-band rejection at close-in and far-out offset frequencies are achieved thanks to the sharp filtering profile from the SAW filter. Also, frequency up-conversion boosts the IF filter order, resulting in increased roll-off slopes in dB/dec. The filter wide bandwidth (65 MHz) is preserved across the entire range. The input-side selectivity is limited by the on-chip LC-tank Q. However, thanks to an all-passive design, the close-in input-referred IP3 is still 24 dB better compared with the state-of-the-art in the same RF range (Table 1).

The measured IB 1-dB compression point (P-1dB) is +6.4 dBm while the IB-IIP3 is +20.3 dBm. At OOB (1×bandwidth offset Δf), blocker-induced 1-dB compression point (B-1dB) of +4.3 dBm and IIP3 of +29.4 dBm are measured (Fig. 9). The OOB linearity is almost independent of Δf as it is dominated by the N-path switches. Advanced

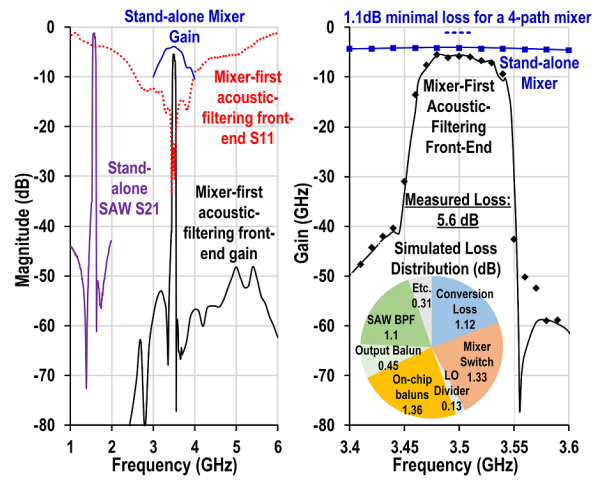


Fig. 7. Measured (lines) and simulated (markers) responses of the mixer-first acoustic-filtering RF front-end and a stand-alone mixer.

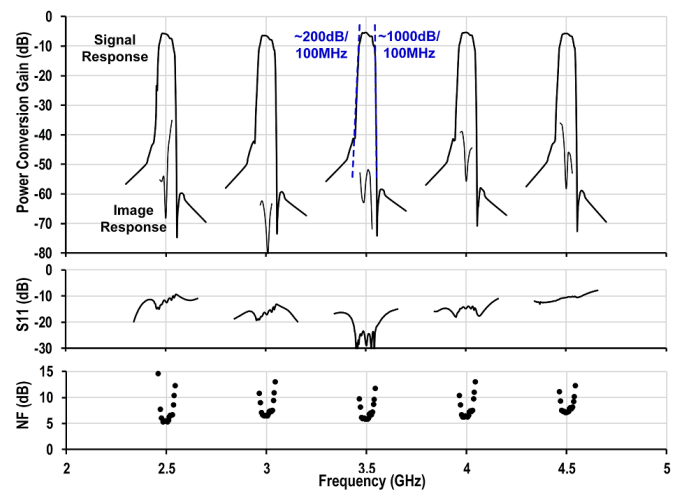


Fig. 8. Measured conversion gain, input matching, and NF of the mixer-first acoustic-filtering RF front-end across frequencies.

technology and high-linearity switch design can be used to improve the linearity and power-handling capability.

IV. CONCLUSION

Table 1 compares this work with state-of-the-art band-pass filter and receivers. When compared with the high-order N-path filter in [1], this work exhibits 33 dB more OOB rejection, operates at 3× higher RF with 5× reducing in average power, while having comparable NF, IB and OOB linearity. Comparing with the frequency-selective receiver in [5], this work has 2-to-3 dB higher NF at 2.5-to-4.5 GHz but exhibits 29 dB more OOB rejection at 1.5×BW offset frequency and 24 dB higher OOB IIP3 at 1×BW while achieving significant power reduction. Comparing with superheterodyne receivers (e.g. [10]), this work exhibits order-of-magnitude higher linearity thanks to the elimination of active devices before filtering.

The proposed mixer-first acoustic-filtering front-end further benefits from advancements of both circuits and acoustic devices. Topics for future research include lowering the NF/loss using advanced technology and a holistic approach

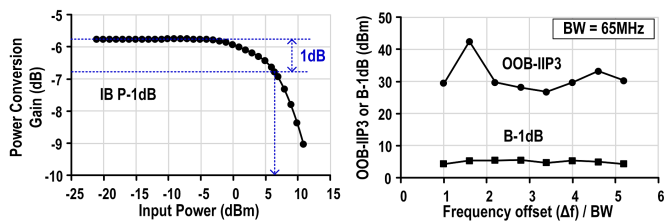


Fig. 9. IB and OOB gain compression and IIP3 measurement results with the RF front-end input tuned at 3.5 GHz.

Table 1. Measurement summary and comparison with state-of-the-art works.

Metric	JSSC 2016 [10]	JSSC 2018 [5]	JSSC 2019 [1]	This work
Topology	Super-Heterodyne Receiver	N-path Mixer-First Receiver	High-Order N- path Filter	Mixer-First Acoustic Filtering
IF (MHz)	Up to 262	0	0	1600
Technology	28nm CMOS	45nm CMOS SOI	65nm CMOS	65nm CMOS + SAW
Tuning Range (GHz)	0.5 ~ 2.5	0.2 ~ 8.0	0.8 ~ 1.1	2.5 ~ 4.5
NF (dB)	2.1 ~ 2.6	3 ~ 4 (2.5-to-4.5GHz RF)	5 ~ 8.6	5.5 ~ 7.1
Peak IB Gain (dB)	35	21 (voltage gain)	-4.6 ~ -3.8 (power gain)	-6.4 ~ -5.4 (power gain)
3dB RF BW (MHz)	6.5 ~ 20	20	30 ~ 50	65
Passband to Stopband Rejection (dB)	20 (Δf=2×BW)	21 (Δf=2×BW)	17 (Δf=1.5×BW)	50 (∆f=1.5×BW, SAW filter dependent)
Filtering Roll-off Slope# (dB/100MHz)	40	80	200 (lower side)/ 100 (higher side)	200 (lower side)/ 1000 (higher side)
OOB-IIP3 (dBm)	+14 (∆f>10×BW)	+5 (∆f=1×BW) or +39 (∆f=8×BW)	+24 (∆f=1×BW)	+29.4 (∆f=1×BW)
IB-IIP3 (dBm)	+2^	0 ~ +5	+25	+20.3
B-1dB (dBm)	N/A	+12 (∆f=8×BW)	9 (∆f=1×BW)	4.3 (∆f=1×BW)
Power (mW)	22 ~ 40 (RX)	131 ~ 191 (RX) (2.5-to-4.5GHz RF)	80 ~ 97 (BPF)	12 ~ 26 (mixer- first frond-end)
Active Area (mm²)	0.52	0.8	2.3	1.4*

estimated from the figure ^ estimated from OOB IIP3 and LNTA only * not including off-chip components

towards the passive recombination network design, enhancing linearity and power handling, as well as scaling the design beyond 6 GHz and into millimeter-wave frequencies.

ACKNOWLEDGMENT

This work was partially supported by NSF under the SpecEES program. The authors would like to thank Integrand EMX for electromagnetic simulation.

REFERENCES

- P. Song and H. Hashemi, "RF Filter Synthesis Based on Passively Coupled N-Path Resonators," IEEE JSSC, 2019.
- [2] N. Reiskarimian and H. Krishnaswamy, "Design of all-passive higher-order CMOS N-path filters," in 2015 IEEE RFIC.
- [3] Y. Yang, R. Lu, and S. Gong, "Scaling Acoustic Filters Towards 5G," in 2018 IEEE IEDM, 2018.
- [4] E. C. Szoka and A. Molnar, "Circuit Techniques for Enhanced Channel Selectivity in Passive Mixer-First Receivers," in 2018 IEEE RFIC.
- [5] Y. Lien, E. A. M. Klumperink, B. Tenbroek, J. Strange, and B. Nauta, "Enhanced-Selectivity High-Linearity Low-Noise Mixer-First Receiver With Complex Pole Pair Due to Capacitive Positive Feedback," *IEEE JSSC*, 2018.
- [6] C. Andrews and A. C. Molnar, "A Passive Mixer-First Receiver With Digitally Controlled and Widely Tunable RF Interface," *IEEE JSSC*, 2010.
- [7] A. Mirzaei and H. Darabi, "Analysis of Imperfections on Performance of 4-Phase Passive-Mixer-Based High-Q Bandpass Filters in SAW-Less Receivers," *IEEE TCAS-I*, 2011.
- [8] P. Warder and A. Link, "Golden Age for Filter Design: Innovative and Proven Approaches for Acoustic Filter, Duplexer, and Multiplexer Design," *IEEE Microwave Magazine*, 2015.
- [9] Data sheet: SAW RF filter Automotive telematics (B3519), Qualcomm.
- [10] I. Madadi, M. Tohidian, K. Cornelissens, P. Vandenameele, and R. B. Staszewski, "A High IIP2 SAW-Less Superheterodyne Receiver With Multistage Harmonic Rejection," *IEEE JSSC*, 2016.